

Embedded coupler based on selectively infiltrated photonic crystal fiber for strain measurement

Ying Wang,^{1,2} C. R. Liao,¹ and D. N. Wang^{1,*}

¹Department of Electrical Engineering, The Hong Kong Polytechnic University, Hong Kong, China

²Laboratory of Optical Information Technology and School of Science, Wuhan Institute of Technology, Wuhan 430073, China

*Corresponding author: eednwang@polyu.edu.hk

Received August 6, 2012; revised October 11, 2012; accepted October 12, 2012;

posted October 12, 2012 (Doc. ID 173899); published November 14, 2012

A photonic crystal fiber (PCF) with embedded coupler is demonstrated for strain measurement. The embedded coupler is constructed by the selective filling of one of the air holes in the PCF. Light propagated in the fiber core can be efficiently coupled to the liquid-filled rod waveguide under phase-matching conditions, resulting in sharp decreasing of resonant wavelength intensity. The highest strain sensitivity is calculated to be ~ 23.8 pm/ $\mu\epsilon$ due to the coupling between core mode and fundamental mode of the liquid rod, when the refractive index (RI) of the liquid is 1.46. With the increase of the RI, the resonance can also be observed between the core mode and the higher-order modes of the liquid rod, whereas the strain sensitivity drops to ~ 6.4 pm/ $\mu\epsilon$. The experimentally obtained static strain sensitivity values are ~ 22 and ~ 3.8 pm/ $\mu\epsilon$ for the coupling between the core mode and the fundamental mode or linearly polarized LP₁₁ modes of the liquid rod, respectively, which are in good agreement with the simulations. The dynamic strain measurement resolution obtained is ~ 1.2 ne/(Hz)^{1/2}. © 2012 Optical Society of America

OCIS codes: 130.2790, 230.3990, 060.2370.

Highly sensitive strain measurement by use of optical fiber sensor has been attractive in many applications such as structural health monitoring, aerospace, and nanotechnology. Such a measurement can be achieved in an active or a passive sensing scheme. A representative of an active optical fiber strain sensor with extremely high sensitivity is based on laser-frequency modulation technique, which has a detection limit of $\sim \text{p}\epsilon$ ($10^{-12}\epsilon$) or lower [1,2]. However, such a system is rather complex. By contrast, a passive sensing scheme is simple, in which fiber interferometers, fiber Bragg gratings (FBGs), and long-period fiber gratings (LPFGs) are widely used, and the sensitivity achieved is typically below 3 pm/ $\mu\epsilon$ for a fiber Mach-Zehnder interferometer [3,4], ~ 1 pm/ $\mu\epsilon$ for an FBG [5,6], and ~ 10 pm/ $\mu\epsilon$ for an LPFG [7].

Recently, optical fiber sensors based on selective infiltration of a photonic crystal fiber (PCF) have been proposed for temperature sensing with extremely high sensitivity up to a few tens of nm/ $^{\circ}\text{C}$, representing a new way of achieving ultrasensitive measurements [8–10].

In this Letter, we propose and demonstrate an ultrasensitive strain sensor based on PCF with embedded coupler structure, formed by selectively filling one of the PCF air holes with refractive index (RI) liquid by use of a femtosecond (fs)-laser-assisted selective infiltration method reported previously [9]. The liquid rod created acts as a waveguide, which, together with PCF fiber core, essentially forms an embedded coupler. By simply changing the RI of the infiltrated liquid, the coupled modes of the device can be selected between the PCF core mode and the fundamental mode or higher-order mode of the liquid rod. The static strain sensitivity obtained in the experiment is ~ -22 pm/ $\mu\epsilon$ for the coupling between the PCF core mode and the fundamental mode of the liquid rod, which agrees well with the simulation result of -23.8 pm/ $\mu\epsilon$ and is superior to that of other passive strain sensing schemes.

The cross-section view of the PCF with embedded coupler is shown in Fig. 1. One of the air holes in the cladding of the PCF (LMA-10, NKT Photonics) is filled

with standard RI liquid (Cargille Laboratories, Inc.). In principle, any air hole in a PCF can be infiltrated to form a liquid rod waveguide. However, different infiltrated air holes lead to different coupling lengths. The operating principle of the proposed sensor can be explained by coupled-mode theory for the directional coupler. The coupling length of the device at a given wavelength is given by $L_c = \pi/(\beta_e^{\sigma} - \beta_o^{\sigma})$, where β_e^{σ} and β_o^{σ} are the propagation constants of the even and odd coupled modes, respectively, and σ denotes the polarization state (x or y polarization, as shown in Fig. 1) [11].

Numerical simulations based on the finite element method (FEM) were performed to quantitatively characterize the PCF with embedded coupler, with hole diameter $d = 3.06$ μm , hole-to-hole spacing $\Lambda = 6.46$ μm , Poisson's ratio $\nu = 0.17$, and axial photoelastic coefficient $C_z = -0.27$. Here the liquid rod was assumed to be not perturbed by axial strain. Moreover, dispersions of fused silica and RI liquids were considered according to the Sellmeier's formula and Cauchy's formula, respectively. Although the Cauchy's formula is precise only for wavelengths between 400 and 700 nm, we can extrapolate them into the near-IR region with reasonable accuracy since the RI liquid used in the experiment exhibits low dispersion. Figure 2(a) shows the phase-matching curves

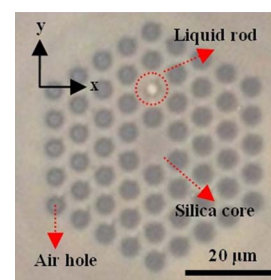


Fig. 1. (Color online) Cross-section view of the selectively infiltrated PCF with embedded couplers. The red dotted circles highlight the hole filled with standard RI liquid.

of the linearly polarized (LP) PCF core mode (core LP₀₁) and the fundamental mode of the liquid rod (rod LP₀₁), both in y polarization, at the temperature of 30°C, with the hole filled with 1.46 RI liquid as shown in Fig. 1. A resonant wavelength of ~ 1485 nm can be determined in Fig. 2(a) with the help of the auxiliary gray dashed lines in the avoided crossing region (marked with green lines in Fig. 2) where the modes existed cannot be identified as the core or the rod modes. This resonance originates from the coupling between the even and odd hybrid modes, and the even mode has a higher effective index than the odd mode over the avoided crossing. By applying an axial strain of 500 $\mu\epsilon$, the resonant wavelength shifts to 1471.6 nm and a strain sensitivity of -23.8 pm/ $\mu\epsilon$ can be obtained. The calculated coupling length is 18.7 mm. The coupling length and the strain sensitivity for x -polarized modes are nearly the same as those of the y -polarized modes. If the location of the infiltrated hole (with the same RI liquids) changes, the strain sensitivity maintains while the coupling length varies. Moreover, a smaller core-to-rod spacing results in a shorter coupling length.

The PCF core mode can also coupled into a higher-order mode of the liquid rod provided that the air hole

is filled with appropriate RI liquid. For instance, the resonance between the core mode and the LP₁₁ mode of the liquid rod can be observed in the near-IR wavelength region by filling the air hole with liquid of RI of ~ 1.50 . Figure 2(b) displays the phase-matching curves of core LP₀₁ and rod LP₁₁ modes, which include TE, TM, and hybrid electromagnetic (HE) modes. Note that the phase-matching curves of x -polarized modes (the combinations of LP_{01x}, HE_{21x}, and TE₀₁ modes) are not shown in Fig. 2(b) for clarity. Resonance I denotes the coupling between the core LP_{01y} and rod HE_{21y} modes, while the coupling between the core LP_{01y} and rod TM₀₁ modes is denoted as Resonance II. The coupling lengths for Resonance I and II are calculated as 29.0 and 27.8 mm, respectively. For the coupling between LP_{01x} and HE_{21x} and between LP_{01x} and TE₀₁, the corresponding coupling lengths are 30.1 and 30.7 mm, respectively. The strain sensitivities for all the mode combination cases mentioned above are calculated as ~ 5.9 pm/ $\mu\epsilon$.

In the experiments, PCF (LMA-10) was infiltrated following the procedures reported in [9]. After infiltration, both ends of the selectively infiltrated PCF were cleaved and fusion spliced with single-mode fibers (SMFs). Standard 1.46 RI and 1.506 RI liquid were used in the experiment, of which the temperature—RI coefficients are -3.89×10^{-4} and -4.02×10^{-4} refractive index unit/°C, respectively. An optical spectrum analyzer and a broadband light source (1250–1650 nm) were used to observe the transmission spectra of the infiltrated PCFs, and a high-precision column oven was used to stabilize the environment temperature of the device in the accuracy of 0.1°C.

Two PCF samples with the infiltrated hole as shown in Fig. 1 were fabricated: sample I was filled with 1.46 RI liquid and had a length of ~ 26 mm, and sample II was filled with 1.506 RI liquid and had a length of ~ 37 mm. Initially, no clear dips but only broad lossy bands were observed in the transmission spectra due to the relatively long infiltrated length. Thus, the samples were cut back to close to their coupling lengths to suppress the over-coupling effect.

Sample I was kept in a column oven at 31.3°C to observe the transmission dip in the wavelength region of the light source. After a 10 min period of temperature stabilization, sample I was stretched along the fiber axis to introduce the axial strain. It can be found from Fig. 3(a) and its inset that the resonant wavelength experiences a blueshift with the increase of strain and there is a linear relationship between the resonant wavelength and the axial strain applied. The average strain sensitivity obtained is ~ -22 pm/ $\mu\epsilon$, while the largest resonant dip depth is >20 dB, with an insertion loss of ~ 11 dB, mainly due to the fusion splicing of PCF and SMF. Figure 3(b) demonstrates the strain sensing characteristics of sample II, which was maintained at 25°C in the column oven.

The average strain sensitivity obtained is ~ 3.8 pm/ $\mu\epsilon$. The inset of Fig. 3(b) shows the transmission spectra of sample II at different strain values. The resonant dip around 1500 nm is due to the coupling between the PCF core LP₀₁ and rod HE₂₁ modes, while the other one around 1520 nm is due to the coupling between the core LP₀₁ and rod TE₀₁ and TM₀₁ modes. According to

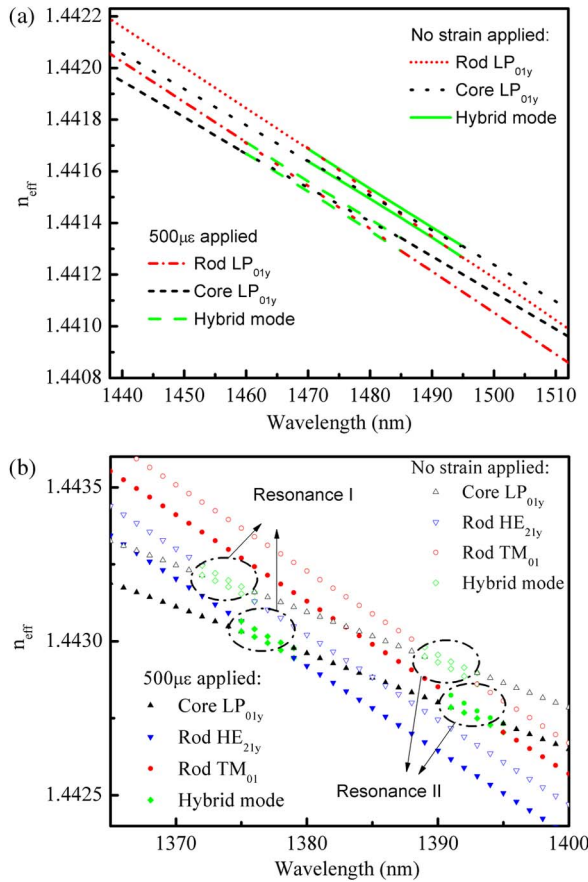


Fig. 2. (Color online) Phase-matching curves of the coupling between the y -polarized PCF core mode (a) fundamental mode and (b) LP₁₁ mode of the infiltrated liquid rod waveguide at 30°C before and after the axial strain is applied. Note that only the HE₁₁, HE₂₁, and TM₀₁ modes are plotted in (b) for clarity, and the avoided crossings between the core LP₀₁ and rod HE₂₁ and between the core LP₀₁ and TM₀₁ modes are denoted as Resonance I and II, respectively.

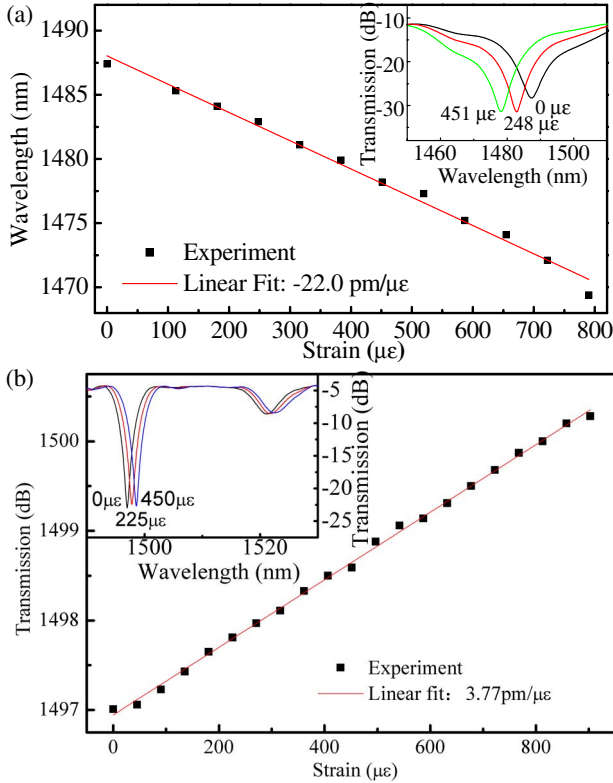


Fig. 3. (Color online) Resonant wavelength shift with applied axial strain for (a) 31.3°C, 1.46 RI liquid filled and (b) 25°C, 1.506 RI liquid filled PCF with lengths of 26 and 37 mm, respectively. The infiltrated holes of the samples are the same as that shown in Fig. 1. Insets show their transmission spectra at different strains.

[12], the detection limit of samples I and II are calculated as 34 and 22 $\mu\epsilon$ by assuming a signal-to-noise ratio (SNR) of 60 dB.

The strain sensitivity obtained in our device is one order higher than that of fiber interferometer and FBG and two or three times larger than that of an LPFG, which can be further enhanced if appropriate RI material can be utilized, as long as the slope of the rod mode dispersion is close to that of the silica core dispersion.

The dynamic strain resolution was also investigated by employing a tunable laser, a photodiode, and an electric spectrum analyzer. Sample II was fixed onto a piezoelectric actuator and kept in a column oven. The dynamic strain applied was 8.3 $\mu\epsilon$, with frequency varied from 100 to 1000 Hz. The Fourier transform of the output at 1000 Hz is shown in Fig. 4, where the resolution bandwidth is 5 Hz and the SNR is over 70 dB, which gives a dynamic strain resolution of $\sim 1.2 \text{ n}\epsilon/(\text{Hz})^{1/2}$.

The device is also highly sensitive to temperature. The temperature sensitivities for samples I and II are measured as $\sim 58 \text{ nm}/^\circ\text{C}$ and $\sim 11 \text{ nm}/^\circ\text{C}$, respectively. Thus, the strain measurement should be implemented in a constant temperature environment.

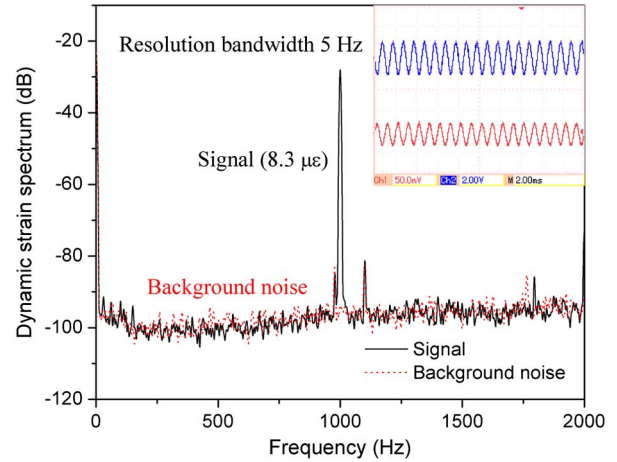


Fig. 4. (Color online) Measured strain resolution spectrum of sample II.

In conclusion, we have demonstrated a strain sensor based on a PCF with embedded coupler, fabricated by use of an fs-laser-assisted selective infiltration technique. A high strain sensitivity of $\sim 22 \text{ pm}/\mu\epsilon$ is obtained for the coupler operated with the PCF core mode and the fundamental mode of the liquid rod, which is in good agreement with the FEM simulation results and is one order higher than that of conventional FBG and fiber interferometer. Such a device has high potential in ultra-sensitive strain measurements.

This work was supported by Hong Kong SAR government GRF grant PolyU 5298/10E and The Hong Kong Polytechnic University grants G-YK58 and 4-ZZE3 and by the National Natural Science Foundation of China under grant 61108016.

References

1. J. H. Chow, D. E. McClelland, M. B. Gray, and I. C. M. Littler, *Opt. Lett.* **30**, 1923 (2005).
2. G. Gagliardi, S. De Nicola, P. Ferrara, and P. De Natale, *Opt. Express* **15**, 3715 (2007).
3. J. Villatoro, V. Finazzi, V. P. Minkovich, V. Pruneri, and G. Badenes, *Appl. Phys. Lett.* **91**, 091109 (2007).
4. L. M. Hu, C. C. Chan, X. Y. Dong, Y. P. Wang, P. Zu, W. C. Wong, W. W. Chan, and T. Li, *IEEE Photon. J.* **4**, 114 (2012).
5. C. Chen, A. Laronche, G. Bouwmans, L. Bigot, Y. Quiquempois, and J. Albert, *Opt. Express* **16**, 9645 (2008).
6. N. Liu, Y. Li, Y. Wang, H. Wang, W. Liang, and P. Lu, *Opt. Express* **19**, 13880 (2011).
7. Y.-P. Wang, L. Xiao, D. N. Wang, and W. Jin, *Opt. Lett.* **31**, 3414 (2006).
8. D. K. C. Wu, B. T. Kuhlmeier, and B. J. Eggleton, *Opt. Lett.* **34**, 322 (2009).
9. Y. Wang, C. Liao, and D. N. Wang, *Opt. Express* **18**, 18056 (2010).
10. Y. Wang, M. Yang, D. N. Wang, and C. R. Liao, *IEEE Photon. Technol. Lett.* **23**, 1520 (2011).
11. J. Lægsgaard, O. Bang, and A. Bjarklev, *Opt. Lett.* **29**, 2473 (2004).
12. I. M. White and X. D. Fan, *Opt. Express* **16**, 1020 (2008).